Supplemental information

In our discussion of zooplankton grazing as a driver of changing phytoplankton variance with anthropogenic warming, we consider the parameterization of zooplankton grazing in the CESM1-LE. The biogeochemical ecosystem model simulates a single generic zooplankton functional type (ZFT) with different grazing rates and half saturation constants prescribed for different PFTs (e.g. slower zooplankton grazing rates for larger phytoplankton). Grazing rate for the single ZFT is computed using a Holling Type III (sigmoidal) relationship:

$$G = g_{max} \cdot T_{lim} \cdot Z \cdot \frac{P^2}{P^2 + K^2} \tag{5}$$

where g_{max} is the maximum grazing rate, T_{lim} is the temperature limitation (Q10) function, Z is the zooplankton concentration, P is the phytoplankton concentration, and K is the half-saturation constant for grazing. Zooplankton loss scales with temperature and a linear mortality term which represents zooplankton losses from predation.

Figure S1 illustrates changes in grazing rate as a function of diatom concentration using this parameterization. To approximate the effects of climatic warming, we plot the relationship for across a series of increasing temperatures: (blue) 5°C, (orange) 10°C, and (green) 15°C. The maximum grazing rate increases with warming temperatures. Changes in diatom concentration in mmol m^{-3} between the beginning and end of the century are denoted by dark and light orange circles, respectively.

To provide context for the CESM1-LE results, we examine changes in chlorophyll variance from a subset of the Coupled Model Intercomparison Project 5 (CMIP5) models (Taylor et al., 2011): the GFDL-ESM2M from the Geophysical Fluid Dynamics Laboratory (GFDL; (Dunne et al., 2012, 2013), the CanESM2 from the Canadian Centre for Climate Modelling and Analysis (Christian et al., 2010; Arora et al., 2011), and the MPI-ESM-LR from the Max Planck Institute (MPI; (Giorgetta et al., 2013; Ilyina et al., 2013), consisting of 30, 50, and 100 ensemble members, respectively. Similarly to the CESM1-LE, historical forcing was applied through 2005, followed by RCP8.5 forcing through 2100.

We compare the variance in chlorophyll observed among the large ensembles to a synthetic ensemble generated from observational chlorophyll concentrations over the MODIS remote sensing record (Elsworth et al., 2020, 2021). A synthetic ensemble is a novel technique that allows the observational record to be statistically emulated to create multiple possible evolutions of the observed record, each with a unique sampling of internal climate variability (McKinnon et al., 2017; McKinnon and Deser, 2018). We use the synthetic ensemble of chlorophyll concentration to compare the variability observed in the real world to the variability simulated across a suite of ESM ensembles.

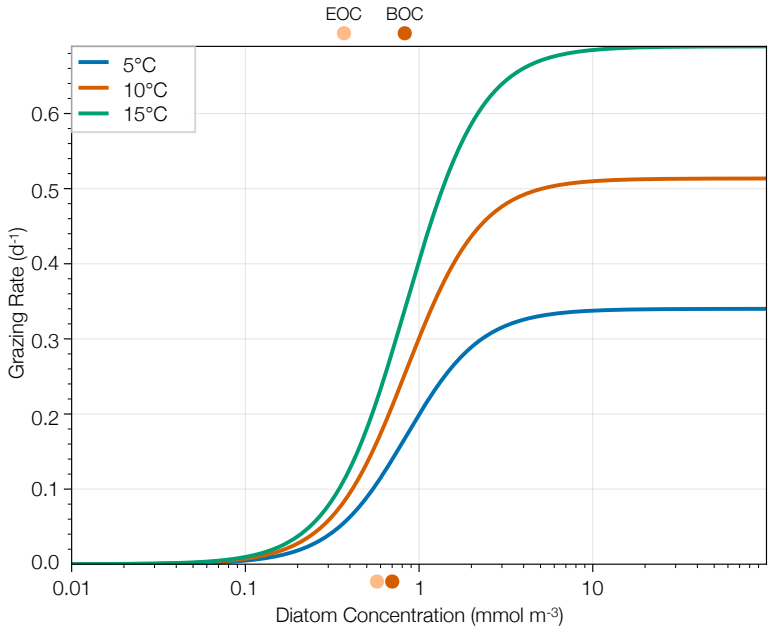

Figure S1. Holling Type III (sigmoidal) functional parameterization of zooplankton grazing rate in the biogeochemical ecosystem model of the CESM1-LE across a range of temperatures. Changes in diatom concentration between the beginning and end of the century (BOC and EOC, respectively) are shown in the dark and light orange circles, respectively, with the changes in the ASP region shown above and changes in the SAP region shown below.

To provide context for Figure 3, we include the spatial distribution of total phytoplankton carbon concentration (Figure S3a) and internal standard deviation in phytoplankton carbon concentration (Figure S3b) simulated by the CESM1-LE across the RCP8.5 forcing scenario (2006 to 2100). Total phytoplankton carbon concentration is relatively high in the subpolar Atlantic and Pacific, the Southern Ocean, and the Eastern Equatorial Upwelling Zone and relatively low in the subtropical gyre regions (Figure S3a). Regions of relatively high phytoplankton carbon concentrations correspond to regions of high variance (Figure S3b).

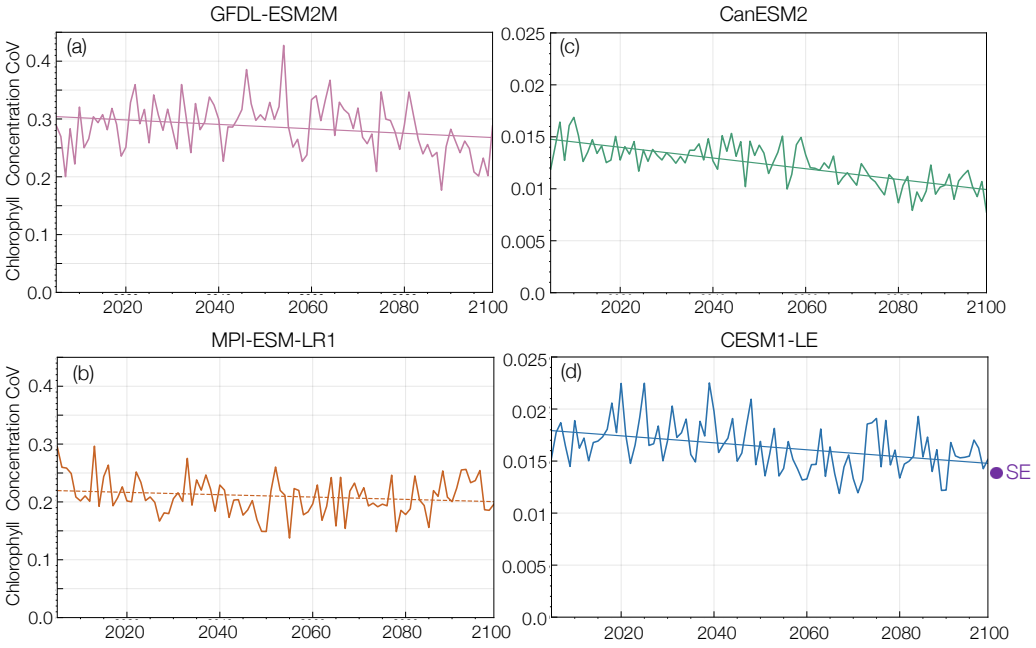

Figure S2. Coefficient of variance (internal standard deviation divided by ensemble mean) in annual mean global surface ocean chlorophyll concentration from 2006 to 2100 across a suite of CMIP5 model ensembles: (a) (pink) GFDL-ESM2M (b) (orange) MPI-ESM-LR1 (c) (green) CanESM2 (d) (blue) CESM1-LE. The average coefficient of variance of the synthetic ensemble (SE) created using the MODIS surface ocean chlorophyll record is shown in the purple dot on the vertical axis (Elsworth et al., 2020, 2021).

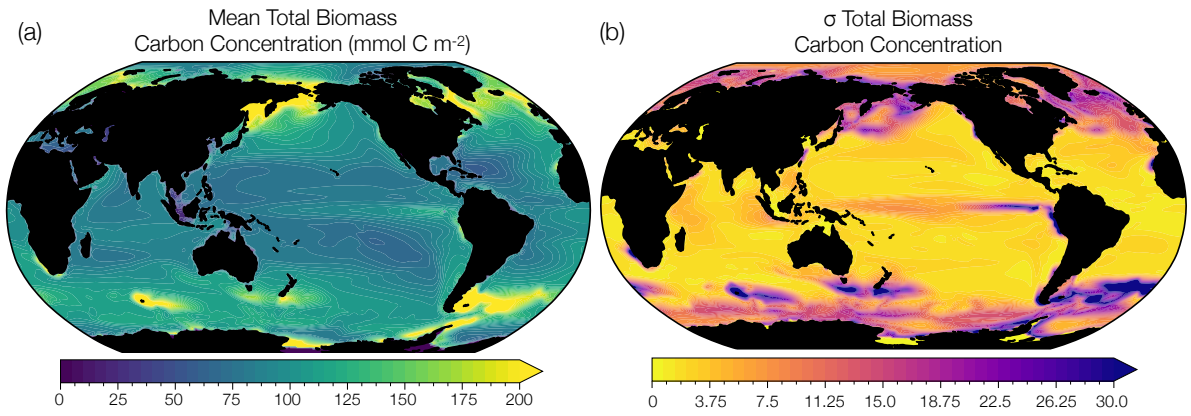

Figure S3. (a) Total phytoplankton carbon concentration simulated by the CESM1-LE in mmol C m^{-2} averaged across the RCP8.5 forcing scenario (2006 to 2100). (b) Internal standard deviation in total phytoplankton carbon concentration averaged over the same period.

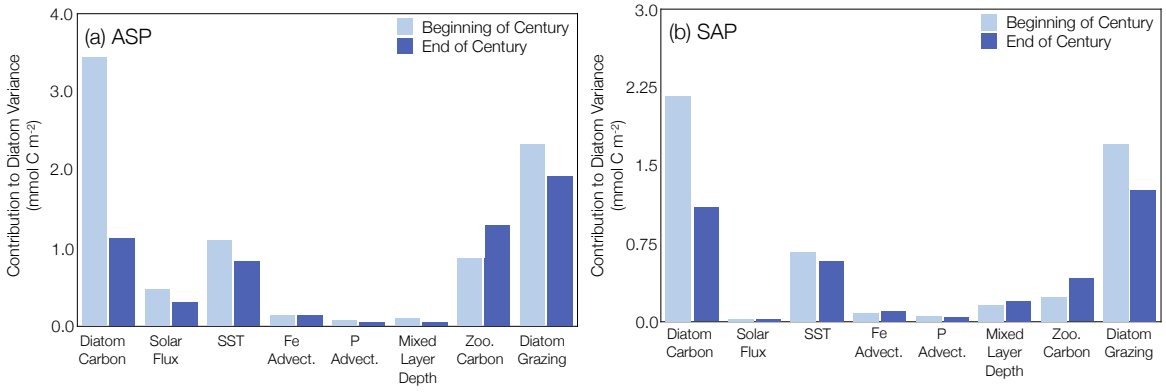

Figure S4. Reconstructed changes in the contribution of each driver variable to phytoplankton biomass variance across the RCP8.5 forcing scenario (2006 to 2100) using variable regression coefficients between the beginning and end of the century. Regions were selected which aligned with the highest fisheries catch in the (a) Atlantic and (b) Pacific basins with the beginning of the century shown in light blue and the end of the century shown in dark blue.

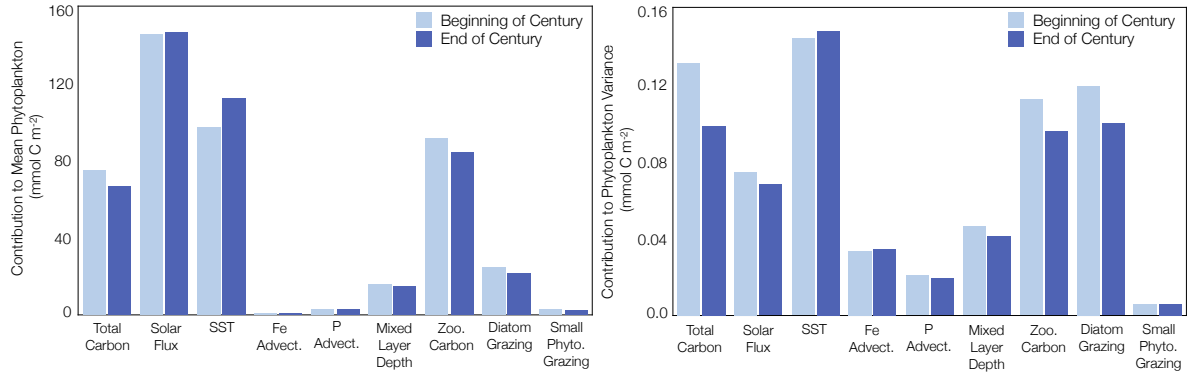

Figure S5. Reconstructed global changes in the contribution of each driver variable to changes in (a) mean phytoplankton biomass and (b) phytoplankton biomass variance across the RCP8.5 forcing scenario (2006 to 2100). The beginning of the century is shown in light blue and the end of the century is shown in dark blue.

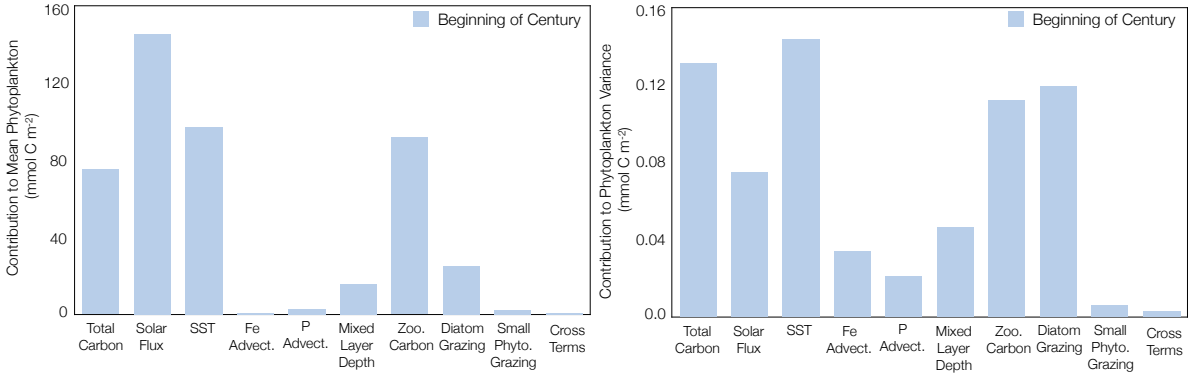

Figure S6. Reconstructed global changes in the contribution of each driver variable to changes in (a) mean phytoplankton biomass and (b) phytoplankton biomass variance across the RCP8.5 forcing scenario (2006 to 2100) across the beginning of the century. The contribution of cross terms to the MLR reconstruction is shown in the rightmost bar in each panel.

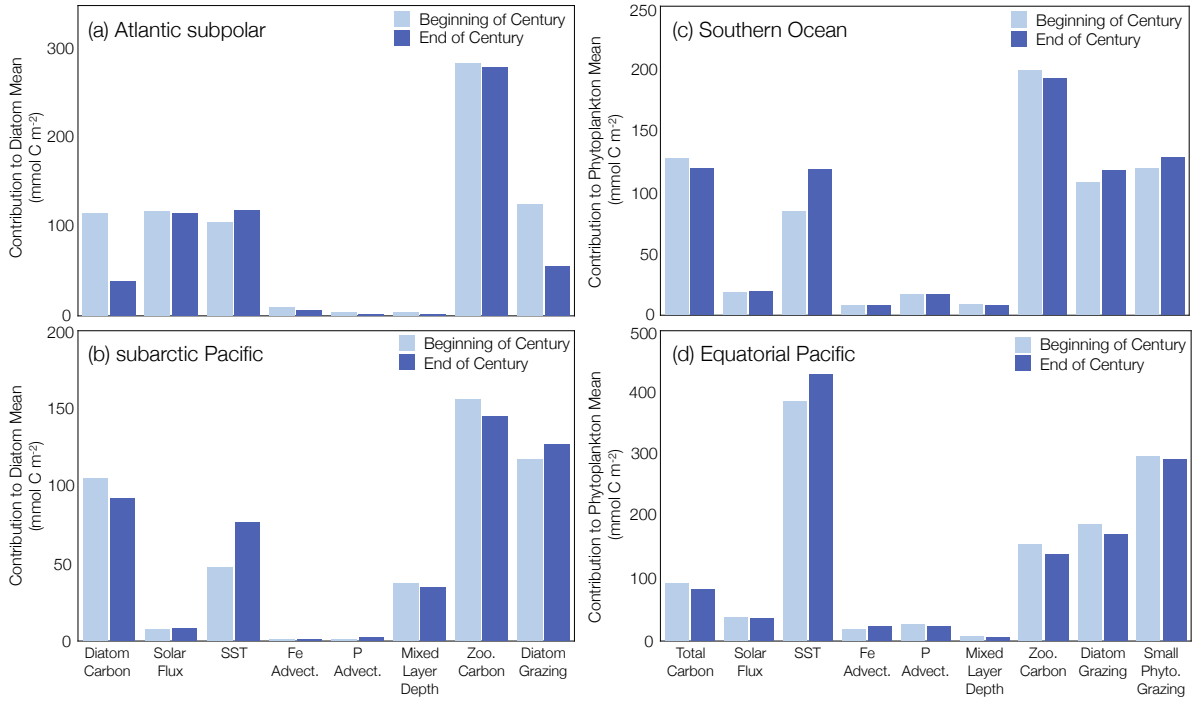

Figure S7. Reconstructed changes in the contribution of each driver variable to mean phytoplankton biomass across the RCP8.5 forcing scenario (2006 to 2100) with the beginning of the century shown in light blue and the end of the century shown in dark blue. Marine ecological regions are defined in Tagliabue et al. (2021). Regions were selected which aligned with the highest fisheries catch in the (a) Atlantic and (b) Pacific basins and the biogeochemically important (c) Southern Ocean and (d) Equatorial Pacific regions. The dominant phytoplankton functional type is considered in each region. In regions with a mixed ecological assemblage, total phytoplankton carbon is considered.

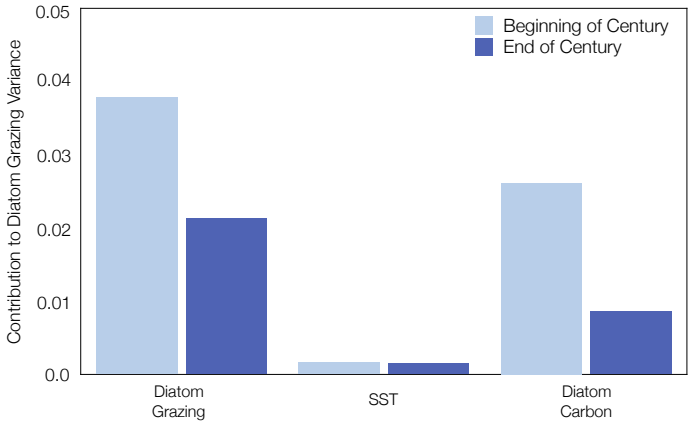

Figure S8. Reconstructed changes in the contribution of sea surface temperature and diatom carbon to changes in diatom grazing variance in the Atlantic supolar (ASP) region across the RCP8.5 forcing scenario (2006 to 2100). The contribution of the change in diatom biomass variance dominates the change in diatom grazing variance.